# HST Palpha Survey of the Galactic Center -- Searching the missing young stellar populations within the Galactic Center

**FULL TITLE**
ASP Conference Series, Vol. **VOLUME**, **YEAR OF PUBLICATION**
**NAMES OF EDITORS**



# HST Pa$\alpha$ Survey of the Galactic Center – Searching the missing young stellar populations within the Galactic Center

H. Dong[1], Q. D. Wang[1], A. Cotera[2], S. Stolovy[3], M. R. Morris[4], J. Mauerhan[3], E. A. Mills[4], G. Schneider[5], C. Lang[6]

[1] *Department of Astronomy, University of Massachusetts, Amherst, MA 01003*

[2] *SETI Institute*

[3] *Spitzer Science Center, California Institute of Technology*

[4] *Department of Physics and Astronomy, University of California, Los Angeles*

[5] *Steward Observatory, University of Arizona*

[6] *Department of Physics and Astronomy, University of Iowa*

*E-mail: hdong@astro.umass.edu, wqd@astro.umass.edu*

**Abstract.** We present preliminary results of our *HST* Pa$\alpha$ survey of the Galactic Center (GC), which maps the central 0.65×0.25 degrees around Sgr A*. This survey provides us with a more complete inventory of massive stars within the GC, compared to previous observations. We find 157 Pa$\alpha$ emitting sources, which are evolved massive stars. Half of them are located outside of three young massive star clusters near Sgr A*. The loosely spatial distribution of these field sources suggests that they are within less massive star clusters/groups, compared to the three massive ones. Our Pa$\alpha$ mosaic not only resolves previously well-known large-scale filaments into fine structures, but also reveals many new extended objects, such as bow shocks and H II regions. In particular, we find two regions with large-scale Pa$\alpha$ diffuse emission and tens of Pa$\alpha$ emitting sources in the negative Galactic longitude suggesting recent star formation activities, which were not known previously. Furthermore, in our survey, we detect ∼0.6 million stars, most of which are red giants or AGB stars. Comparisons of the magnitude distribution in 1.90 $\mu$m and those from the stellar evolutionary tracks with different star formation histories suggest an episode of star formation process about 350 Myr ago in the GC.

## 1. Motivation

As the closest galactic nucleus, the GC (8kpc, [1]) is a unique lab to study resolved stellar populations around a supermassive black hole (SMBH). This topic was triggered by the discovery of three young massive compact star clusters within 30 pc around Sgr A* in the last two decades ($<$ 6 Myr old, $\sim 10^4$ $M_\odot$, [2, 3, 4] and references therein). These clusters contribute strong UV radiation that illuminates nearby molecular clouds. The existence of these clusters provides us with a good opportunity to understand the star formation process within a galactic nucleus, which is very important to the study of galaxy formation and evolution.

However, the formation mechanism of these clusters ([5,6]) still remains greatly uncertain, under the hostile GC environment, characterized by high temperature gas as well as strong magnetic field and tidal force. Existing studies are focused on the Arches

and Center clusters ([7,8]). This small sample of massive stellar clusters prevents us from making a firm conclusion about their formation mode. We do not even know whether they were formed in a single burst or were just part of a continuous star formation in the GC. We are also not sure about whether or not these extreme massive star clusters represent the only way in which stars form in the GC. A survey of a fair sample of massive stars will thus be very helpful.

We also need to determine the long-term star formation history in the GC. Figer et al 2004 ([9]) first studied the K-band luminosity function toward the GC obtained by the HST/NICMOS NIC2. They found that a continuous star formation is consistent with their data. Their conclusion, however, is based on stars detected in several regions with small fields of view. Existing large-scale near-IR surveys, such as 2MASS ([11]), are dominated by foreground stars, plus a limited number of bright red giants and AGB stars in the GC. Therefore, it is highly desirable to have a large-scale, high-resolution near-IR survey, which will facilitate a study of differential properties of the luminosity function across the GC.

We have carried out a HST/NICMOS Pa$\alpha$ survey of the Galactic Center ([10]). This survey used the NIC3, which has a relatively large field of view (51.2"$\times$51.2") and an angular resolution ($\sim$0.2"). This combination, together with the stable PSF, allows us to effectively separate the point sources contribution from the extended diffuse Pa$\alpha$ emission. Arising chiefly from photo-ionized warm gas, Pa$\alpha$ line emission (at 1.87$\mu$m) is brighter than Br$\gamma$ (2.16$\mu$m, accessible from the ground) by a factor of 3-4, even considering the high extinction toward the GC. In particular, point-like Pa$\alpha$ emission should be predominantly produced by evolved massive stars (e.g., O If, LBV and WR) with age younger than $\sim$10 Myr.

## 2. Observation and Data Reduction

Our survey covered the central 416 square arcminutes of the GC in 144 *HST* orbits. Two narrow-band filters, F187N (1.87 $\mu$m, on line) and F190N (1.90 $\mu$m, off line) were used with the same orbit parameters. Each orbit included four pointing positions. Each was observed with a four-point dithering pattern. The exposure time is 192 s for each position and filter.

We will present in Dong et al 2010 ([12]) a detailed description of the data calibration and analysis procedures. Here, we list several key steps. We remove the relative background offsets among the 576 positions simultaneously determined from the detected intensity differences in the overlap regions. The absolute background is determined and removed based on the intensities observed toward several foreground dark molecular clouds. The relative spatial offsets among the orbits are corrected for in the same fashion, while the absolute astrometry is determined from a comparison with the accurate positions of the SiO masers in Reid et al 2007.

We use the IDL routine 'Starfinder' developed by Emiliano Diolaiti ([13]) to detect stars. The 50% completeness limit of the detection is typically $m_{1.90\mu m}$=17 and is reduced to $m_{1.90\mu m} \sim 15$ magnitude near Sgr A*, where faint source confusion becomes important. We are also able to quantify the photometric errors, accounting for the Poisson uncertainty, the background fluctuation, and the NIC3's inter-pixel problem. In total, we detect $\sim$0.6 million sources at 5$\sigma$ confidence in both filters.

We then produce an extinction map calculated adaptively from local flux ratios of sources in the two filters. We use this extinction map to correct for the spatial variable

extinction of the Pa$\alpha$ emission. We further excise individual Pa$\alpha$ sources to construct a diffuse Pa$\alpha$ emission map, which is present in Fig. 1, together with the final F187N and F190N mosaics.

## 3. Result

### 3.1. Magnitude Distribution

In the left panel of Fig. 2, we present a magnitude distribution of the 0.6 million sources in F190N. This distribution shows two peaks at ∼15.5 and 17 magnitudes. While the later peak could be explained by the variable incompleteness of the source detection, the former one should be real, which cannot be due to extinction variation across the field, for example. To understand the nature of the 15.5 magnitude peak, we compare the F190N magnitude contours with the Padova stellar evolutionary tracks in the right panel of Fig. 2. The F190N contours are calculated from the ATLAS 9 atmosphere model and corrected for the distance and extinction ($A_V = 31.1$). As shown by the figure, most of the detected sources should be red giants and AGB stars. Only Main Sequence stars more massive than $\sim 9M_\odot$ should be detected individually in our survey. The peak around 15.5 magnitude is apparently due to red clump stars with initial mass around 1-3 $M_\odot$.

Fig. 3 presents the magnitude distributions constructed for eight different regions. The magnitude distributions of the foreground stars in Regions 3, 4 and 8 show shifts to the dim side because of the presence of foreground molecular clouds. Similarly, the low star number density of Region 5 can be accounted for by the presence of the 50 km/s molecular cloud (M-0.13-0.08). In the remaining 4 regions, the peak around 15.5 magnitude appears to become increasingly more prominent in the regions closer to Sgr A* (cf. Region 1 and 2) and to the Galactic Plane (cf. Region 6 and 7).

### 3.2. Pa$\alpha$ emitting sources

In Fig. 1, we mark the positions of the sources that show significant Pa$\alpha$ emission. These sources are defined from their large ratios of fluxes in the F187N and F190N bands, corrected for local extinction ([12]). 79 of the 157 Pa$\alpha$ sources are apparently located in the three clusters, including most of the evolved massive stars identified spectroscopically (e.g., O If, LBV and WR stars). The remaining sources appear to be distributed outside of these three clusters or in the field. Two third of these field Pa$\alpha$ sources fall in regions between the Arches/Quintuplet and Sgr A*, while the other one third are located on the negative Galactic longitude side. A small fraction of the field Pa$\alpha$ sources are clearly associated with extended HII regions.

### 3.3. Diffuse Pa$\alpha$ emission

Fig. 4 presents three sample regions that show distinct diffuse Pa$\alpha$ emission features at the full resolution. Around Sgr A*, one can clearly see a bright swirling structure, as was discovered by Scoville et al. 2003 ([14]). But in addition, Fig. 4a shows low surface brightness filaments which are nearly perpendicular to the Galactic Plane, which may be an indication for outflows from the very central region around Sgr A*. The well-known radio-thermal filaments in the Sickle nebula and Thermal Arc are now resolved into many thin filaments, which are apparently illuminated by the Arches and Quintuplet clusters (Fig. 4b,c). The Sickle nebula, in particular, shows several

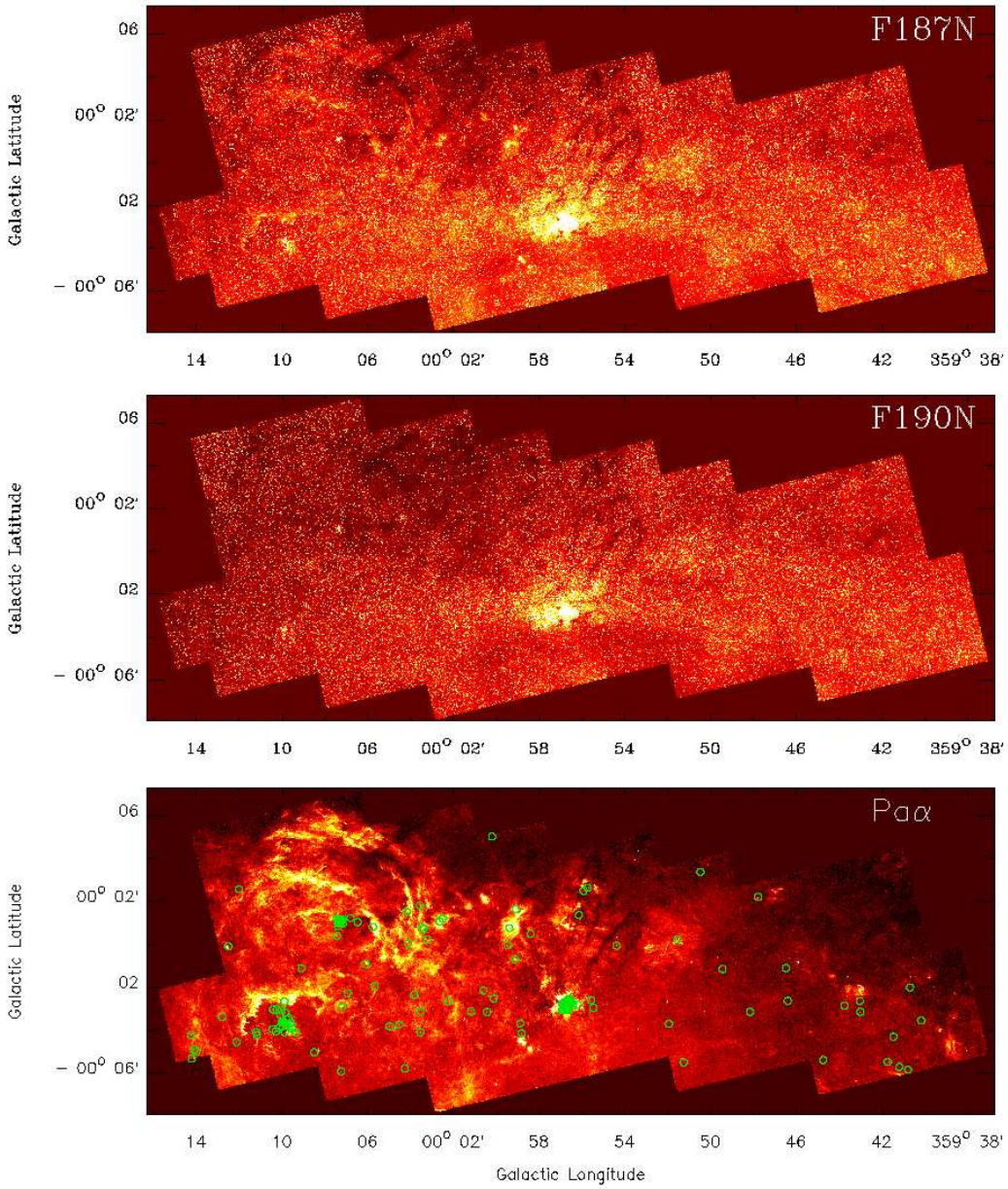


Figure 1. The mosaics from our survey: F187N (top), F190N (middle) and diffuse Pa$\alpha$ emission (bottom). The green circles in the Pa$\alpha$ mosaic mark the positions of the detected Pa$\alpha$ emitting sources (see Section 6).

finger-like structures similar to those seen in M16. But there are also many fuzzy, low surface brightness structures between the Quintuplet cluster and the bright rims. On the Galactic west side of the Sickle nebula, one can also see a new ring-like Pa$\alpha$ nebula. Follow-up spectroscopic observations (Mauerhan et al 2010, in preparation) show that the central Pa$\alpha$ source is an LBV star, similar to the Pistol star.

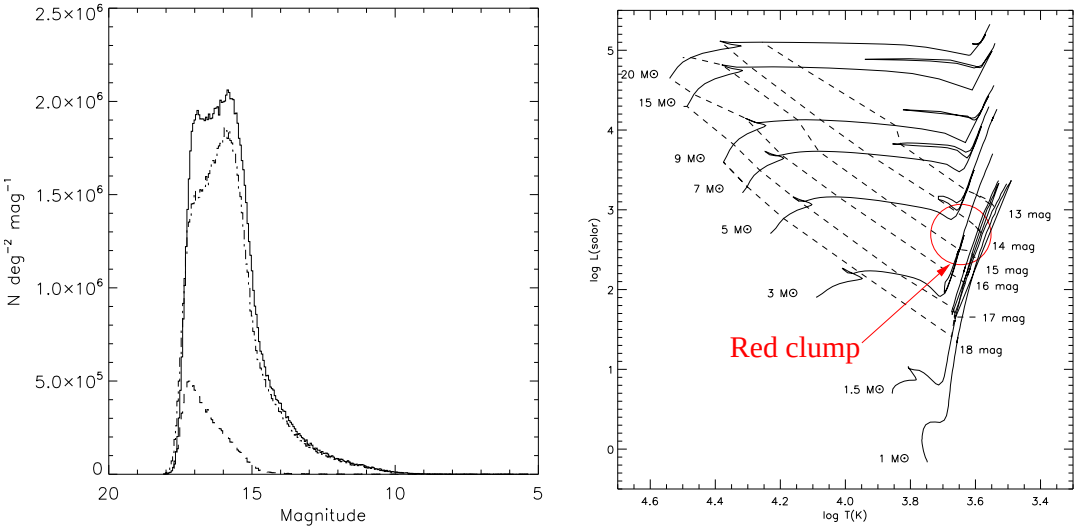


Figure 2. Left: The magnitude distribution of f190N sources. The solid histogram represents the magnitude distributions of all sources, while the dashed and dash-dotted ones are for the foreground (defined to have the color H-K<1 ) and the remaining (GC) sources, separately. Right: The Padova stellar evolutionary tracks with the F190 magnitude contours are overlaid.

Our survey reveals many new Pa$\alpha$ nebulae too. For example, on the negative Galactic longitude side, we find two new extended HII regions at (l,b)=(-0.13,0.0) and (-0.28,-0.036). Compared to the Thermal Arc, they are much dimmer. That is why these regions do not stand out against the strong background in the *Spitzer IRAC* 8 $\mu$m PAH image. Another interesting discovery is the existence of various linear filaments in the two H II regions. These filaments probably trace local magnetic field. We give the full resolution close-ups of extended Pa$\alpha$ emission in Fig. 5. The upper row shows the interaction between the stars and its surrounding ISM. Nebulae in the middle row are probably due to stellar ejecta. Nebulae in the bottom row are several structures that are known as thermal radio sources and are now well resolved. For example, Sgr A-A and Sgr A-C exhibit clear bow shock structures.

## 4. Discussion

### 4.1. How do the massive stars shape the ISM?

Intense ionizing radiation from the three massive star clusters clearly illuminates, erodes and destroys nearby molecular clouds. Our Pa$\alpha$ mosaic provides examples for all these three processes. As shown in Section 3.3., the thin filaments are brighter toward the Arches and Quintuplet clusters, which presents the direct evidence that they are ionizing the surface of the surrounding giant molecular clouds. The finger-like structures at the surface of the Sickle nebula hint that the radiation from the Quintuplet cluster is shaping the ISM, while the fuzzy Pa$\alpha$ features between the Sickle nebula

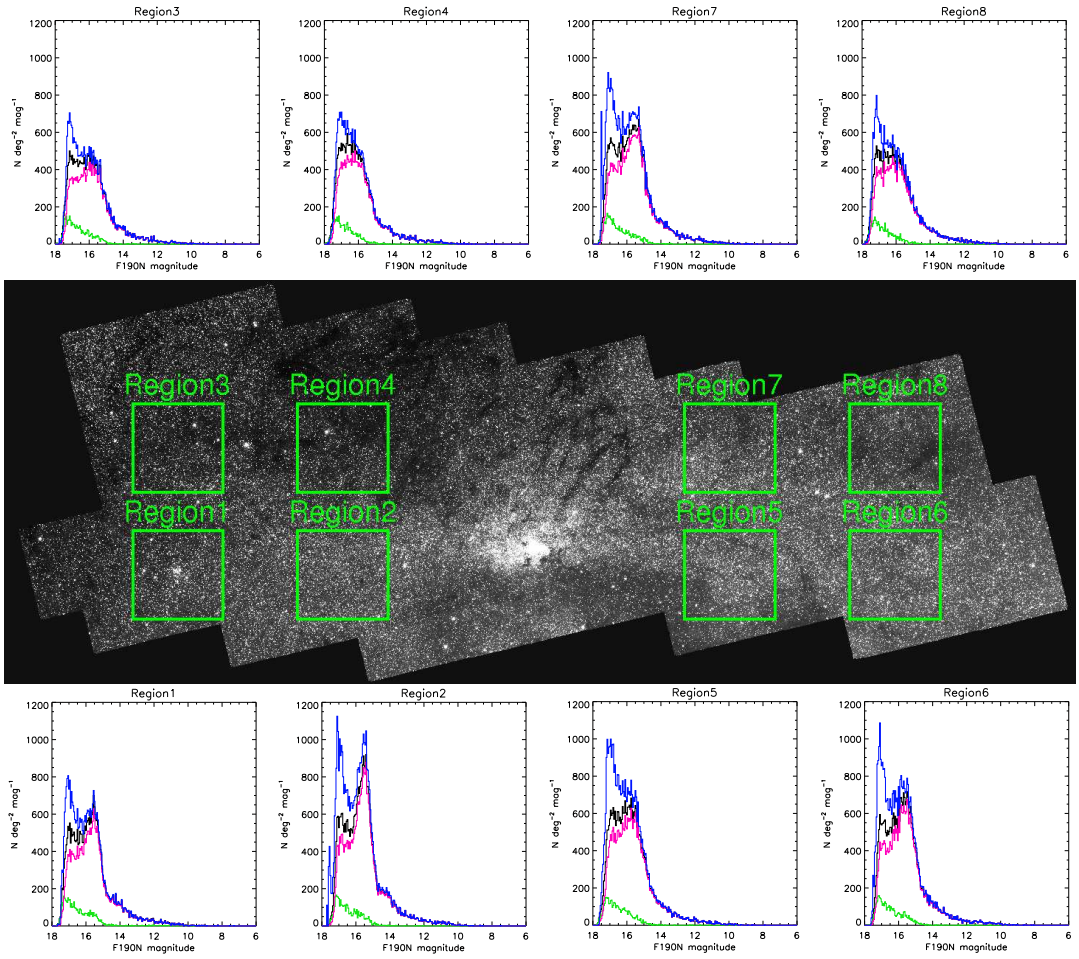


Figure 3. Outlines of the regions in the F190N mosaic that are used to extract the magnitude distributions shown in the individual panels. The black line in each panel represents the original magnitude distribution, while the green and pink lines are for the foreground star and remaining (GC) contributions. The blue line is for the GC distribution after the detection incompleteness correction.

and Quintuplet clusters probably represent remnants of molecular clouds that have already been largely dispersed.

### 4.2. What is the origin of the field Pa$\alpha$ sources

We find that many of the Pa$\alpha$-emitting stars are located outside of the three young massive star clusters. As we mentioned previously, they are evolved massive stars with ages of a few Myr. Studying their origin can help us understand the star formation mode within the GC.

Two third of these field Pa$\alpha$ stars are located on the positive Galactic longitude side of Sgr A* and are close to the three massive star clusters. Stolte et al 2008 ([7]) have found that the Arches cluster is moving toward the Galactic east in a direction parallel to the Galactic plane. In Fig. 1, one can see that there are several Pa$\alpha$ sources

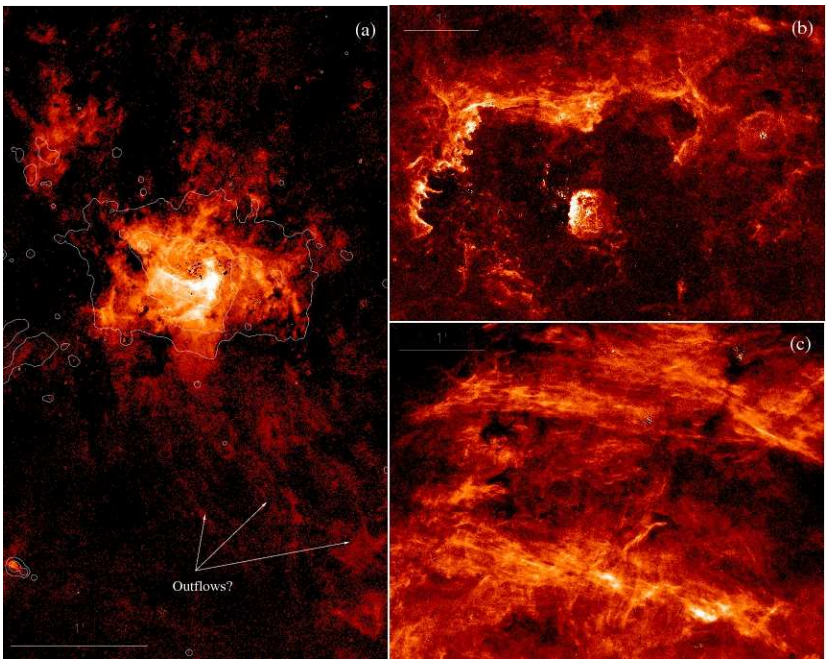


Figure 4. Close-ups of distinct diffuse P$\alpha$ features: (a) the central region around Sgr A*, with the overlaid *IRAC* 8$\mu$m intensity contours at 1,3,10, and 30 $\times 10^3$ mJy sr$^{-2}$; (b) the Sickle nebula; (c) Thermal Arched filaments. All are projected in the Galactic coordinates.

that appear in the opposite direction of the motion. So one possible scenario is that these Pa$\alpha$ sources are ejected from the clusters. Because of the mass segregation, massive stars tend to sink into the cluster centers, where three-body encounters are frequent, leading to ejections of stars and formation of tightly bound binaries. So some of the Pa$\alpha$ sources could be due to the dynamic ejection, although detailed simulations are needed to determine the efficiency of the process and the distribution of such ejected stars. X-ray observations have further shown the presence of three bright X-ray point sources in the Arches cluster ([15] and reference therein). These sources have hard thermal spectra, which are most likely due to colliding winds in individual binaries [15]. Assuming that these three X-ray sources represent all tightly bound binaries of massive stars with strong winds, one may conclude that there should be only a few massive stars at most that may be kicked out from the cluster. Stolte et al 2008 ([7]) also suggested that at most 15% of the total mass may have been stripped away from the Arches cluster by the tidal force in the GC. Due to the mass segregation, the fraction of the massive stars stripped from the cluster should be even smaller. Therefore, the cluster may not be a primary source of the field Pa$\alpha$ sources. Most of the field Pa$\alpha$ sources probably formed in isolation or in small groups, independent of the Arches or Quintuplet cluster.

### 4.3. Current star formation process

Fig. 1 shows that some of the field Pa$\alpha$ sources are associated with extended Pa$\alpha$ diffuse nebulae, which represent regions of massive star formation in small groups.

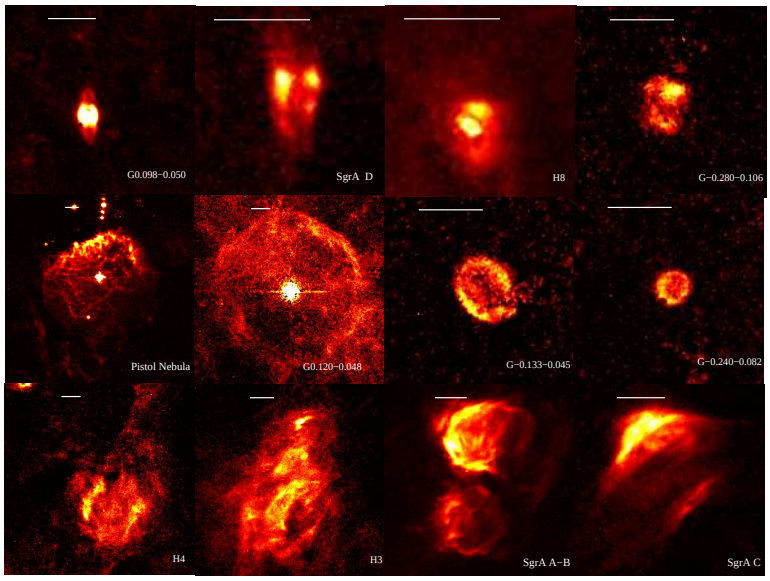


Figure 5. Close-ups of various compact Pa$\alpha$ nebulae (equatorially projected). Detected sources have been subtracted, except for identified bright Pa$\alpha$ emission stars that appear to be central sources of the nebulae. Approximate Galactic coordinates are used as labels of the nebulae, except those with well-known names. The bar in each panel marks a 0.2 pc scale at the GC distance.

These regions cannot be too young because of the presence of the evolved massive stars represented by the Pa$\alpha$ sources. The star groups also cannot be very rich, because of substantially fewer such sources than in the Arches cluster, which has more than 10 $Pa\alpha$-emitting sources within 10" radius. Another evidence for the low mass of the groups is the small sizes and relatively low diffuse Pa$\alpha$ intensities of the nebulae.

Our survey also for the first time unambiguously reveals the presence of two large-scale HII complexes on the negative Galactic longitude side, These complexes, together with the presence of tens of Pa$\alpha$ sources strongly indicates recent star formation on this side of the Galactic disk. Overall, however, the star formation is substantially less active than that on the positive side. One possibility is that the star formation on the negative side preceded the positive one; i.e., clusters/groups have largely been resolved.

Additional evidence for the star formation on the negative side comes from radio observations. Law 2010 ([16]) have shown that a giant Galactic Center lobe of size $\sim$100 pc is not centered at the GC, but shifts to the negative side. This shift may be due to a strong starburst on this side about several Myr ago, responsible for the lobe. Clearly, more observations and detailed modelling are required to further the understanding of the global recent star formation pattern in the GC.

### 4.4. Star formation history

Fig. 6 compares the magnitude distribution in 1.9$\mu$m with a stellar population synthesis model. This comparison shows that the overall shape of the distribution can be reasonably modelled with a constant star formation rate, plus a major burst about 350 Myr ago. The large deviation of the distribution from the model at the small mag-

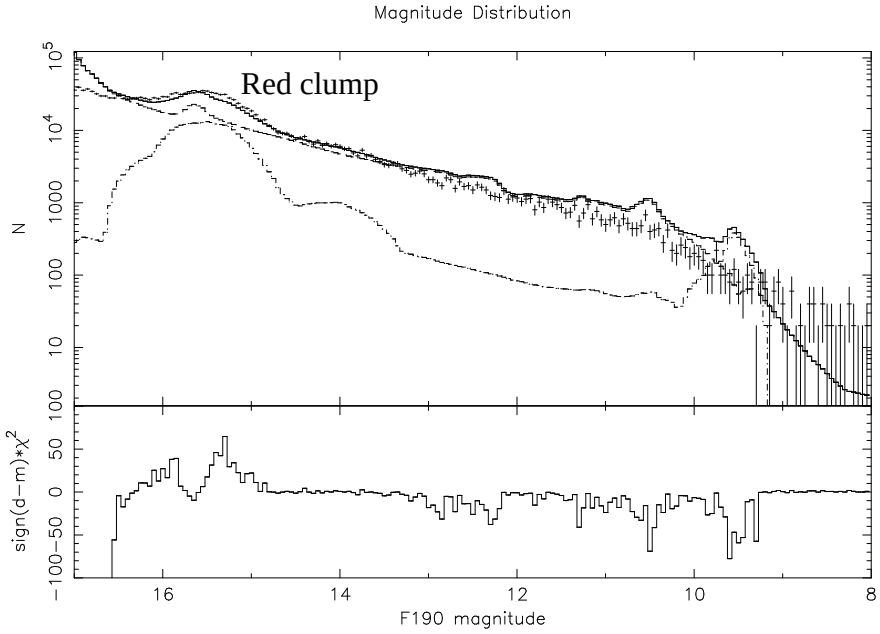


Figure 6. Top: the fitting result. The three lines from bottom to up are the recent star formation activity which began ∼350 Myr ago, the continuous star formation through the whole history of the Universe and their combination. Bottom: the fitting residuals

nitude end is probably caused by a problematic treatment of TP-AGB phase, which has been calibrated with stellar clusters in the Magellanic Clouds. This evolutionary phase may be sensitive to the metallicity, which could be substantially different in the GC from the calibration clusters. The burst in the magnitude distribution model is required to explain the presence of the $m_{1.90\mu m} \sim 15.5$ peak in the data, representing red clump stars with initial mass around 2 $M_{\odot}$. The magnitude position of this peak varies among different lines-of-sight (Fig. 3), which hints that this component is indeed in the GC, not the spiral arms. This spatial variation of the peak intensity further suggests that the distribution of the red clump stars may follow a disk-like structure. While a detailed investigation of the magnitude distribution is yet to be made, it is clear that it can be used to shed important insights into the star formation history in the GC.

## 5. Summary

Based on our *HST* Pa$\alpha$ survey of the GC, we have detected 0.6 million stars and mapped out many extended Pa$\alpha$ emission features. The main results from our preliminary analysis of these products are summarized in the following:

- We have identified 157 Pa$\alpha$-emitting sources. They are most likely evolved massive stars and trace very recent star formation in the GC. About half of the sources are located outside the three well-known massive star clusters. These

field sources formed probably mostly in small groups. Some of the sources are still associated with relatively compact H II regions.

- The diffuse Pa$\alpha$ map allows us to resolve many fine structures in known large-scale thermal radio features in the GC. These structures represent various stages of the interplay between massive stars and their ISM environment, including stellar mass ejection as well as the ionization and destruction of nearby molecular clouds. The filamentary morphology of some of the structures further indicates that magnetic field plays an important role in shaping the ISM in the GC.

- We have clearly detected two HII complexes as well as $\sim$20 Pa$\alpha$ sources on the negative Galactic longitude side, suggesting recent star formation there, though probably earlier and/or weaker than that on the other side. The star formation may be linked to be partly responsible for the GC lobe, as identified by Law et al 2010 ([16], and reference therein).

- We have found evidence for a starburst about 350 Myr years ago, as characterized by an enhanced number of red clump stars evolved from initial masses $\sim$2 $M_{\odot}$. These stars seem to be primarily located in a disk-like region around Sgr A*.

These preliminary results demonstrate that near-IR surveys can be used to significantly advance our understanding of the mode and history of star formation in the GC, shedding insights into what may occur in nuclear regions of other galaxies.

**References**


[1] Ghez, A. M., Salim, S., Weinberg, N. N., Lu, J. R., Do, T., Dunn, J. K., Matthews, K., Morris, M. R., Yelda, S., Becklin, E. E, et al., 2008, ApJ, 689, 1044G
[2] Figer, Donald F., McLean, Ian S., Morris, Mark 1999, ApJ, 514, 202F
[3] Figer, Donald F., Kim, Sungsoo S., Morris, Mark, Serabyn, Eugene, Rich, R. Michael, McLean, Ian S., 1999, ApJ, 525, 750F
[4] Genzel, R., Schödel, R., Ott, T., Eisenhauer, F., Hofmann, R., Lehnert, M., Eckart, A., Alexander, T., Sternberg, A., Lenzen, R., et al., 2003, ApJ, 594, 812G
[5] Fujii, M., Iwasawa, M., Funato, Y., Makino, J.,2008, ApJ, 686, 1082F
[6] Nayakshin, S., Cuadra, J., Springel, V., 2007, MNRAS, 379, 21
[7] Stolte, A., Ghez, A., Morris, M., Lu, J., Matthews, K., 2008, ApJ, 675, 1278S
[8] Paumard, T., Genzel, R., Martins, F., Nayakshin, S., Beloborodov, A. M., Levin, Y., Trippe, S., Eisenhauer, F., Ott, T., Gillessen, S., 2006, ApJ, 643, 1011P
[9] Figer, D. F., Rich, R. M., Kim, S. S., Morris, M., Serabyn, E., 2004, ApJ, 601, 319F
[10] Wang, Q. D., Dong, H., Cotera, A., Stolovy, S., Morris, M., Lang, C. C., Muno, M. P., Schneider, G., Calzetti, D., 2009, MNRAS, tmp, 1865W
[11] Skrutskie, M. F., Cutri, R. M., Stiening, R., Weinberg, M. D., Schneider, S., Carpenter, J. M., Beichman, C., Capps, R., Chester, T., Elias, J. et al., 2006, AJ, 131, 1163S
[12] Dong, H., Wang, Q. D., Cotera, A., Stolovy, S., Morris, M., Lang, C. C., Muno, M. P., Schneider, G., Calzetti, in preparation
[13] Diolaiti, E., Bendinelli, O., Bonaccini, D., Close, L., Currie, D., Parmeggiani, G., 2000, A&AS, 147, 335D
[14] Scoville, N. Z., Stolovy, S. R., Rieke, M., Christopher, M., Yusef-Zadeh, F. 2003, ApJ, 594, 294
[15] Wang, Q. D., Dong, H., Lang, C., 2006, MNRAS, 371, 38
[16] Law, C. J., 2010, ApJ, 708, 474